BIOCHEMISTRY
including biophysical chemistry & molecular biology

Article

pubs.acs.org/biochemistry

Glucocorticoid Receptor–DNA Dissociation Kinetics Measured *in Vitro* Reveal Exchange on the Second Time Scale

Rolando W. De Angelis,[†] Nasib K. Maluf,[†,§] Qin Yang,[†] James R. Lambert,[‡] and David L. Bain*[,†]

[†]Department of Pharmaceutical Sciences and [‡]Department of Pathology, University of Colorado Anschutz Medical Campus, Aurora, Colorado 80045, United States

ABSTRACT: The glucocorticoid receptor (GR) is a member of the steroid receptor family of ligand-activated transcription factors. Recent live cell imaging studies have revealed that interactions of GR with chromatin are highly dynamic, with average receptor residence times of only seconds. These findings were surprising because early kinetic studies found that GR–DNA interactions *in vitro* were much slower, having calculated residence times of minutes to hours. However, these latter analyses were conducted at a time when it was possible to work with only either partially purified holoreceptor or its purified but isolated DNA binding domain. Noting these limitations, we reexamined GR–DNA dissociation kinetics using a highly purified holoreceptor shown to be amenable to rigorous study. We first observe that GR–DNA interactions *in vitro* are not slow as previously thought but converge with *in vivo* behavior, having residence times of only seconds to tens of seconds. This rapid exchange is seen at six individual response elements and the multisite MMTV promoter used in live cell imaging. Second, GR dissociation rates are identical for all response elements. Thus, previously observed differences in receptor affinity toward these sequences are not due to differences in off rate but in on rate. Finally, dissociation kinetics are biphasic in character. A minimal kinetic model consistent with the data is that in which DNA-bound GR interconverts between states on a second time scale, with dissociation occurring via a multistep process. We speculate that receptor interconversion in this time frame can be recognized by the coregulatory proteins that interact with GR, leading to unique transcriptional responses.

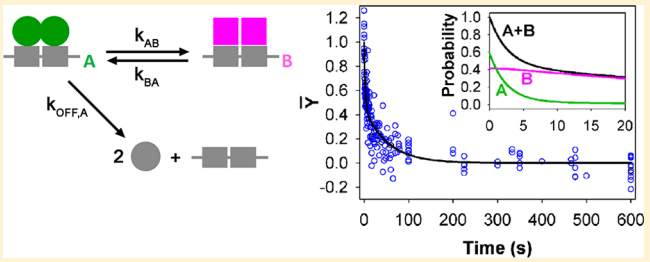

The glucocorticoid receptor (GR) is a member of the steroid receptor family of ligand-activated transcription factors.[1] Upon binding ligand, the receptor activates gene expression by first assembling at hormone response elements (HREs), typically as a dimer. Receptor–DNA binding is coupled to recruitment of coregulatory proteins, chromatin remodeling, and transcriptional activation. Advances in live cell imaging have allowed visualization of a subset of these events *in vivo*, with the finding that GR interactions with chromatin are highly dynamic. For example, initial studies using an engineered array of the mouse mammary tumor virus (MMTV) promoter revealed an average GR residence time of only 10 s.[2] More recent studies of receptor interactions at single-copy, endogenous promoters have also reported fast exchange.[3]

Rapid exchange *in vivo* was surprising because early *in vitro* work had demonstrated that GR–DNA interactions were much slower. For instance, kinetic dissociation studies using full-length GR and the MMTV promoter resolved an off rate of 1.1×10^{-4} s^{-1}, corresponding to an average residence time of 2.5 h.[4] Similar results were seen using only the GR DNA binding domain (DBD) and a single HRE, resolving an off rate of 2.2×10^{-4} s^{-1} or an average residence time of 1.3 h.[5] This discrepancy between *in vitro* and *in vivo* GR binding dynamics led to the proposal that in live cells, the receptor is actively displaced from DNA as a part of the chromatin remodeling process.[6]

Although the *in vitro* studies described above were once state of the art, they were also conducted at a time when it was possible to study only either the partially purified holoreceptor or the purified but isolated DBD. The advent of baculovirus–insect cell expression systems has now allowed high-yield expression and purification of intact GR, which in turn has facilitated more detailed biophysical investigations. These studies have revealed that the highly purified holoreceptor displays a number of attributes not seen with unpurified GR or its isolated domains. These include differences in receptor assembly state, DNA binding energetics, cooperative assembly at complex promoters, and the role of such interactions in regulating transcription *in vivo*.[7,8] In light of these developments, and noting that live cell imaging studies are not yet positioned to gain physical mechanisms of receptor–DNA interactions, we decided to reexamine *in vitro* GR dissociation kinetics. Our goal was to shed additional light on the kinetic mechanisms by which the GR holoprotein interacts with its response elements and multisite promoters. As shown in Figure 1a, we analyzed a series of six well-characterized response elements,[7,9] and the MMTV promoter used in live cell imaging (Figure 1b).[2]

Received: June 20, 2015
Revised: August 12, 2015
Published: August 12, 2015

DOI: 10.1021/acs.biochem.5b00693
Biochemistry 2015, 54, 5306–5314

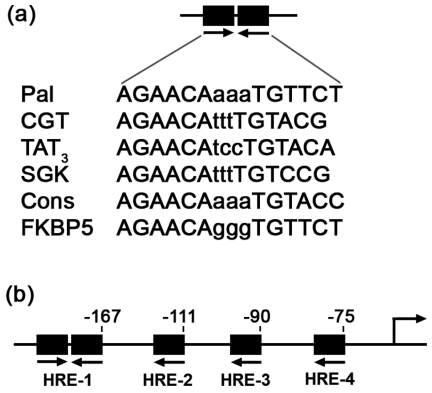

Figure 1. Schematics for six response elements and the mouse mammary tumor virus (MMTV) promoter. (a) Sequences for the six palindromic-like HREs. Half-sites are represented by black rectangles; arrows indicate the relative orientation. (b) Response elements located in the MMTV promoter. Arrows below the schematic represent the relative orientation. Numbers represent the upstream distance from the transcriptional start site, noted as an arrow above the schematic. Site 1 represents a GTTACAaaaTGTTCT sequence. Sites 2−4 represent half-sites with a TGTTCT sequence.

Our studies reveal that GR−DNA interactions *in vitro* are not slow as previously thought but converge with *in vivo* behavior, with GR residence times of only seconds to tens of seconds. Rapid exchange is observed at all response elements and the MMTV promoter. We also find that GR dissociation rates are identical for all response elements tested, indicating that previously observed differences in receptor binding affinity toward these sequences are not due to differences in off rate but in on rate. Finally, we observe that GR−DNA dissociation kinetics are biphasic in character. A minimal kinetic model consistent with all data is that the DNA-bound receptor interconverts between states on a second time scale, resulting in a multistep dissociation process. We speculate that interconversion within this time frame can be recognized by the coregulatory proteins that interact with GR, leading to unique transcriptional responses.

MATERIALS AND METHODS

Expression and Purification of Full-Length Human GR. Detailed protocols for expressing and purifying full-length GR have been described previously.[7,8] Briefly, the receptor is expressed as a hexahistidine-tagged protein in baculovirus-infected insect cells. The nuclear lysate is fractionated over Ni^{2+}-agarose resin, followed by Sephacryl S-300 size exclusion chromatography. Eluted GR is then concentrated using Q-Sepharose. A similar approach was used to express and purify a glucocorticoid−estrogen receptor chimera (GR/ER) used here as a control protein, in which the ligand binding domain of GR is substituted with that of human estrogen receptor-α.[10] Saturating levels of the ligands triamcinolone acetonide (for GR) or 17-β-estradiol (for GR/ER) were present throughout receptor expression, purification, and storage. Receptor concentrations were determined using calculated extinction coefficients of 71280 M^{-1} cm^{-1} for GR and 52830 M^{-1} cm^{-1} for GR/ER.[11]

Sedimentation Velocity Analysis. Sedimentation velocity of GR was conducted as described previously, using a Beckman Optima XL-A analytical ultracentrifuge.[7,8] The buffer consisted of 20 mM Tris-HCl (pH 8.0 at 4 °C), 100 mM NaCl, 1 mM $CaCl_2$, 2.5 mM $MgCl_2$, 1 mM DTT, and 10 μM TA. GR was sedimented at 1.5 μM, 50000 rpm, and 4 °C. Data were collected at 230 nm. Sedimentation coefficient $c(s)$ distributions were determined using Sedfit.[12]

Quantitative Equilibrium Footprinting. Equilibrium footprints were conducted as described by Ackers and coworkers[13] with minor modifications.[14] Footprinting was conducted using a 1100 bp DNA fragment containing the TAT_3 imperfect palindrome (see Figure 1a). Buffer conditions were identical to those in the sedimentation velocity studies, with the addition of 100 μg/mL BSA and 2 μg/mL salmon sperm DNA. Binding isotherms were generated as previously described[13,14] using ImageQuant (Molecular Dynamics).

Quantitative Kinetic Footprinting. Kinetic footprints were conducted as described by Beckett and Brenowitz[15,16] with minor modifications. As an example, the 1100 bp radiolabeled DNA fragment described above containing the TAT_3 sequence was equilibrated at a single GR concentration under buffer conditions identical to those described for equilibrium footprinting. Once equilibrium had been reached, a 45 μL aliquot was transferred to a tube containing 5 μL of unlabeled HRE-containing DNA at a 1−100-fold molar excess over GR (hereafter termed "trap"). The sample was then allowed to incubate for times ranging from 2 to 600 s. After the desired amount of time, 45 μL of the sample was transferred to a tube containing 5 μL of 0.6 unit/μL DNase and allowed to react for exactly 3 s. DNase digestion was stopped by adding 45 μL of 20 mM EDTA, and the sample was processed as described previously.[14] This approach, when conducted over a range of trap incubation times, generated a single kinetic decay curve. We then repeated this process over a range of initial GR concentrations, for five additional HREs, and the MMTV promoter (Figure 1). Trap concentrations covering a 1−100-fold molar excess over GR concentration generated identical dissociation kinetics, indicating that reassociation of GR to the radiolabeled DNA was not occurring and therefore only GR−DNA dissociation was being monitored.

Resolution of Observable Rate Constants. All kinetic decay curves were first fit to a single-exponential model:

$$\bar{Y} = Ae^{-k_{obs}t} \quad (1)$$

where $\bar{Y}$ is the fractional saturation of the DNA at time t, A is the amplitude, and k_{obs} is the observable rate constant. Noting that all time courses also showed visual evidence of biphasic decay, we also fit them to a double-exponential model:

$$\bar{Y} = A_1e^{-k_{obs,1}t} + A_2e^{-k_{obs,2}t} \quad (2)$$

where A_1 and A_2 are the amplitudes of the fast and slow phases, respectively, and $k_{obs,1}$ and $k_{obs,2}$ are their respective rate constants. Time courses were analyzed via nonlinear least squares using Scientist (Micromath, Inc.). An F-test at the 95% confidence level was used to determine whether the double-exponential fit was statistically improved compared to the single-exponential fit.[17]

Molecular Interpretation of Biphasic Kinetics. Biphasic kinetics are indicative of a multistep dissociation process. A minimal kinetic model that best describes the data posits that the GR−DNA complex exists as an equilibrium between two interconverting states, A and B, with only state A dissociating from the DNA. As shown in Figure 9a, this model is defined by dissociation rate constant $k_{off,A}$ and interconversion rate constants k_{AB} and k_{BA}. Using this model, we globally fit 11 GR decay curves for the TAT_3 sequence using the following ordinary differential equations:

DOI: 10.1021/acs.biochem.5b00693
Biochemistry 2015, 54, 5306−5314

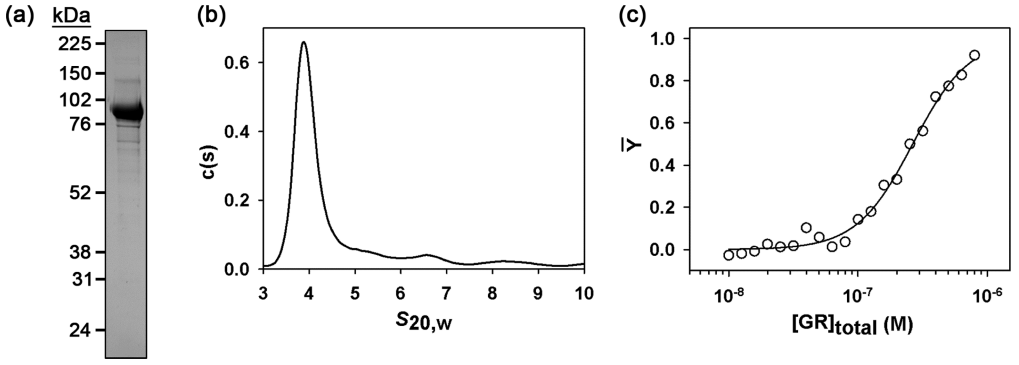

Figure 2. Purification and biophysical characterization of full-length human GR. (a) Coomassie-stained sodium dodecyl sulfate−polyacrylamide gel electrophoresis image of 5 μg of purified GR. (b) Sedimentation coefficient distribution of 0.5 μM GR determined by Sedfit analysis.[12] (c) Fractional saturation ($\bar{Y}$) of the TAT_3 response element by GR determined by quantitative equilibrium footprinting. The solid line represents the best fit to a contracted Adair equation.[8]

$$\frac{d[D_f]}{dt} = k_{off,A}[GR_2D]_A \quad (3)$$

$$\frac{d[GR_2D]_A}{dt} = -(k_{AB} + k_{off,A})[GR_2D]_A + k_{BA}[GR_2D]_B \quad (4)$$

$$\frac{d[GR_2D]_B}{dt} = k_{AB}[GR_2D]_A - k_{BA}[GR_2D]_B \quad (5)$$

where $[D_f]$ is the time-dependent concentration of free DNA, $[GR_2D]_A$ is the time-dependent concentration of the GR−DNA dimer complex in state A, and $[GR_2D]_B$ is the time-dependent concentration of the complex in state B. At the start of dissociation, we set $[D_f] = 0$, $[GR_2D]_A = 1/(1 + k_{AB}/k_{BA})$, and $[GR_2D]_B = 1 - [GR_2D]_A$. The expressions for $[GR_2D]_A$ and $[GR_2D]_B$, now expressed as fractions relative to each other, ensure that both states are in equilibrium at time zero. Finally, the experimental observable, the fractional saturation as a function of time $[\bar{Y}(t)]$, is equal to the time-dependent probability of the two states:

$$\bar{Y}(t) = \frac{[GR_2D]_A + [GR_2D]_B}{[D]_f + [GR_2D]_A + [GR_2D]_B} \quad (6)$$

Because the kinetic experiments were conducted over a range of GR concentrations, resulting in a range of initial $\bar{Y}$ values, all time courses were treated as transition curves (Y_{app}) with upper (m) and lower (b) end points:

$$\bar{Y}(t)_{app} = (m - b) \times \bar{Y}(t) + b \quad (7)$$

For the purpose of presentation, all decay curves shown herein were normalized to $\bar{Y}$ values ranging from 0 to 1. Differential equations were solved implicitly using Scientist (Micromath, Inc.).

RESULTS

Full-Length GR Is Amenable to Kinetic Analysis. We recently developed protocols for high-yield expression and purification of full-length human GR.[7,8] We further showed that the purified receptor is structurally and functionally homogeneous and, therefore, amenable to thermodynamic studies. Here we reproduce a portion of these findings to lend credence to our kinetic investigations. As shown in Figure 2a, the full-length receptor can be purified to >90% as judged by densitometry. As shown in Figure 2b, sedimentation velocity studies indicate that GR sediments primarily as a 4.2 S species with a molecular mass of 90 kDa. This agrees with the calculated mass of the GR monomer (90925 Da) and is consistent with our more comprehensive sedimentation studies demonstrating that GR shows no evidence of self-association up to and above micromolar concentrations. (The remaining species from 5 to 10 S reflect small amounts of irreversible GR aggregates we believe to be functionally inactive.[8]) Shown in Figure 2c is an equilibrium binding isotherm for GR assembly at the TAT_3 response element. The total binding affinity was determined to be $(1.1 \pm 0.2) \times 10^{13}$ M^{-2} or −16.5 kcal/mol, indicating that GR binds with strong affinity. Separate fitting to a Hill equation resolved a Hill coefficient of 1.8 ± 0.2, indicating substantial cooperativity between the two bound monomers. All of these findings are statistically identical to the results of our previous studies using both His-tagged and FLAG-tagged GR[7,8] and suggest that the receptor purified here is amenable to detailed kinetic analysis.

GR−Response Element Dissociation Kinetics Are Biphasic and Occur on the Second Time Scale. We first studied GR dissociation kinetics at the TAT_3 response element. Shown in Figure 3a is a kinetic footprint showing dissociation of GR from this sequence over 600 s. The resultant decay curve is shown in Figure 3b, with the first 50 s shown in the inset. Visual inspection indicates that the half-life for the GR−DNA complex is between 10 and 20 s, comparable to the short residence time seen in live cells. Fitting to a single-exponential decay model (dotted line) resolved an observed rate constant, k_{obs}, of 0.025 s^{-1}. However, the single-exponential model poorly describes the data, particularly in the first 50 s of dissociation (Figure 3b, inset). We therefore fit the data to a double-exponential or biphasic decay model, which resulted in a visually improved fit over the entire time course (solid line). An F-test, which accounts for additional fitting parameters in the biphasic model, confirmed that the fit is statistically improved over the single-exponential fit. The biphasic fit resolved a fast phase rate constant ($k_{obs,1}$) equal to 0.3 ± 0.1 s^{-1} and a slow phase rate constant ($k_{obs,2}$) equal to 0.010 ± 0.002 s^{-1}. These values translate to average GR−DNA residence times of 4 and 100 s, respectively. Finally, the amplitude of each phase was comparable, with a 40% contribution from the fast phase and a 60% contribution from the slow phase.

To further probe the basis of GR−DNA dissociation, we repeated the experiment described above using GR concentrations ranging from 0.14 to 1.4 μM. These concentrations

DOI: 10.1021/acs.biochem.5b00693
Biochemistry 2015, 54, 5306−5314

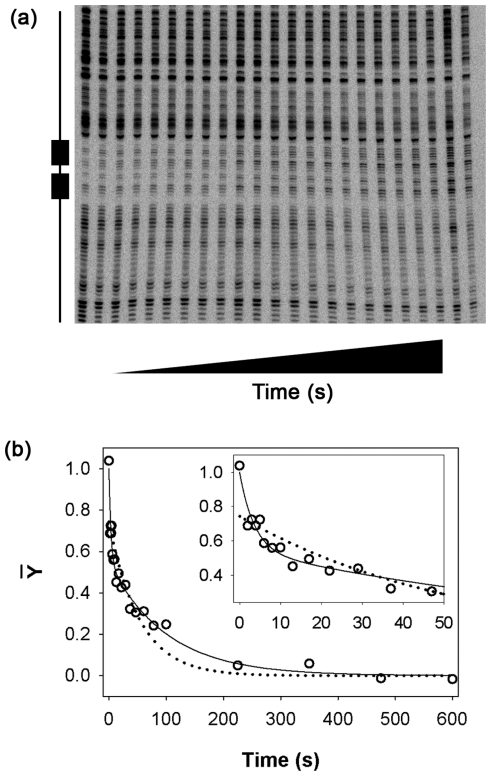

Figure 3. Kinetic footprint and decay curve for dissociation of GR from the TAT_3 response element. (a) Representative autoradiogram of dissociation of GR from the TAT_3 sequence. The GR concentration was 1.4 μM. The position of the binding site is indicated by the schematic at the left. The exposure time to unlabeled competitor DNA increases from left to right as indicated by the triangle. (b) Decay curve determined from analysis of the footprint image in panel a. Empty circles represent the time-dependent GR occupancy at the TAT_3 response element. The dotted line represents the best fit to a single-phase exponential decay model. The solid line represents the best fit to a biphasic decay model. Shown in the inset is a fit covering the first 50 s of GR dissociation.

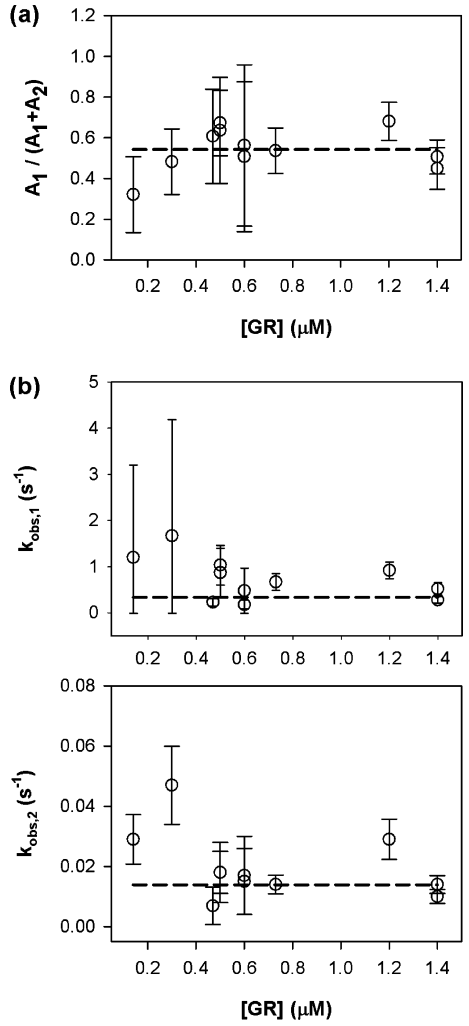

Figure 4. Relative amplitudes and observed rate constants for concentration-dependent GR dissociation from the TAT_3 response element. (a) Empty circles represent the amplitude of the fast phase, A_1, expressed as the $A_1/(A_1 + A_2)$ ratio. Error bars represent the standard deviation propagated from error in both amplitude terms. The dashed line represents the weighted-averaged amplitude across all GR concentrations (0.5 ± 0.1). (b) Observed rate constants and standard deviations for $k_{obs,1}$ and $k_{obs,2}$ as determined from a biphasic decay model. Dashed lines represent the weighted averages across all GR concentrations, calculated to be 0.3 ± 0.2 and 0.014 ± 0.006 s^{-1}, respectively.

correspond to equilibrium GR–DNA occupancies ranging from 0.2 to >0.9 fractional saturation units (see Figure 2c). All time courses were visually similar to that in Figure 3b (not shown), and fitting of the biphasic model again resulted in statistically improved fits. As shown in Figure 4a and Table 1, the resultant amplitude terms [plotted as the $A_1/(A_1 + A_2)$ ratio] show no evidence of GR concentration dependence. A similar result is seen for the two observable rate constants (Figure 4b and Table 1). This lack of concentration dependence indicates that only a single ligation species is present on the DNA regardless of GR concentration. This is the predicted result on the basis of the strong cooperativity seen for GR–DNA binding in the equilibrium studies and suggests that only a GR dimer exists on the DNA in the kinetic studies.

GR–DNA Dissociation Kinetics Are Independent of HRE Sequence. GR binds to a variety of HREs and with a wide range of affinities.[7,9] To determine if the results seen for TAT_3 were recapitulated on other HREs and to address the kinetic basis for differences in GR binding affinity at these sequences, we analyzed receptor dissociation kinetics at the five remaining HREs shown in Figure 1a. The resultant decay curves are shown in Figure 5. Following our approach for analyzing the TAT_3 sequence, we again fit each dissociation curve to either a single- or double-exponential decay model. We found that for all HREs, the biphasic decay model resulted in a statistically improved fit. The resultant fast and slow phase rate constants, $k_{obs,1}$ and $k_{obs,2}$, respectively, for all sequences examined are shown in Figure 6 and Table 2. Surprisingly, we see that neither rate constant changes as a function of GR binding affinity, even though affinity at these sequences covers a 80-fold range.[7] Thus, the GR–DNA binding affinity at these sequences is not controlled by differences in off rate but instead by differences in on rate.

GR Exchange with the MMTV Promoter Also Occurs on the Second Time Scale. We next examined the kinetics of dissociation of GR from the MMTV promoter used in live cell imaging studies. As shown in Figure 1b, this promoter contains one imperfect palindrome (HRE 1) and three recognizable half-sites (HREs 2–4). The GR binding stoichiometry at each site has not been definitively established, although early studies

DOI: 10.1021/acs.biochem.5b00693
Biochemistry 2015, 54, 5306–5314

Table 1. Observed Rate Constants and Relative Amplitudes for Biphasic Dissociation of GR from the TAT_3 Response Element[a]

[GR] (μM)	$k_{obs,1}$ (s^{-1})	$k_{obs,2}$ (s^{-1})	$A_1/(A_1 + A_2)$
0.14	1.2 (−2, +2)	0.029 ± 0.008	0.3 ± 0.2
0.30	1.7 (−1.7, +2.5)	0.047 ± 0.01	0.5 ± 0.2
0.47	0.23 ± 0.08	0.007 ± 0.006	0.6 ± 0.2
0.50	0.9 ± 0.5	0.02 ± 0.01	0.6 ± 0.3
0.50	1.0 ± 0.4	0.018 ± 0.007	0.7 ± 0.2
0.60	0.2 ± 0.1	0.02 ± 0.01	0.5 ± 0.4
0.60	0.5 ± 0.5	0.017 ± 0.01	0.6 ± 0.4
0.73	0.7 ± 0.2	0.014 ± 0.003	0.5 ± 0.1
1.20	0.9 ± 0.2	0.029 ± 0.007	0.70 ± 0.09
1.40	0.28 ± 0.07	0.010 ± 0.002	0.4 ± 0.1
1.40	0.52 ± 0.1	0.014 ± 0.003	0.5 ± 0.1

[a]Parameters were resolved by individually fitting each progress curve (n = 1) to a two-phase exponential decay model using Scientist. Errors represent 68% confidence limits determined via fitting.

suggested that dimers bound at all sites.[4] Shown in Figure 7a is the decay curve for dissociation of GR from the imperfect palindrome (HRE 1), and shown in Figure 7b is the curve for its nearest half-site (HRE 2). Both decay curves were analyzed using single- and double-exponential decay models. On the basis of visual inspection and an F-test, we again find that GR dissociation at each site is statistically best described using a biphasic decay model (solid lines in Figure 7a,b). For site 1, we resolved a fast phase rate constant of 0.9 ± 0.2 s^{-1} and a slow phase rate constant of 0.040 ± 0.009 s^{-1}. Comparable values were seen for site 2, with fast and slow rate constants of 1.0 ± 0.3 and 0.025 ± 0.008 s^{-1}, respectively. Although quantification was not reliable for sites 3 and 4 because of background noise, visual inspection indicated that GR dissociation rates were similar to those observed for sites 1 and 2. In summary, dissociation of GR from the MMTV promoter follows kinetics similar to those seen for individual HREs.

A GR/ER Chimera Also Displays Rapid and Biphasic Dissociation. To eliminate the possibility that our results were an artifact of our GR preparations, we measured the dissociation kinetics of a GR chimera, in which the ligand binding domain of GR is substituted with that of estrogen receptor-α (Figure 8a). The chimera exhibits numerous functional differences compared to GR, including differences in dimerization energetics, transcriptional activity, and cooperativity between nonadjacent binding sites,[10] yet as shown in Figure 8b, dissociation of GR/ER from the TAT_3 response element is again best described by a two-phase exponential decay model. The resolved fast and slow phase rate constants are also similar to those of GR, with $k_{obs,1}$ and $k_{obs,2}$ corresponding to 0.7 ± 0.2 and 0.014 ± 0.004 s^{-1}, respectively. Analysis of dissociation of GR/ER from a subset of the HREs in Figure 1 revealed statistically identical results (not shown). Collectively, our results indicate that biphasic dissociation kinetics are intrinsic to GR and GR/ER. From a mechanistic perspective, the results also indicate that molecular basis of biphasic decay is not obviously linked to the GR hormone binding domain.

DISCUSSION

GR−DNA Interactions Occur on Similar Time Scales both *in Vitro* and *in Vivo*. We report here that GR interactions with DNA are transient *in vitro*; receptor residence

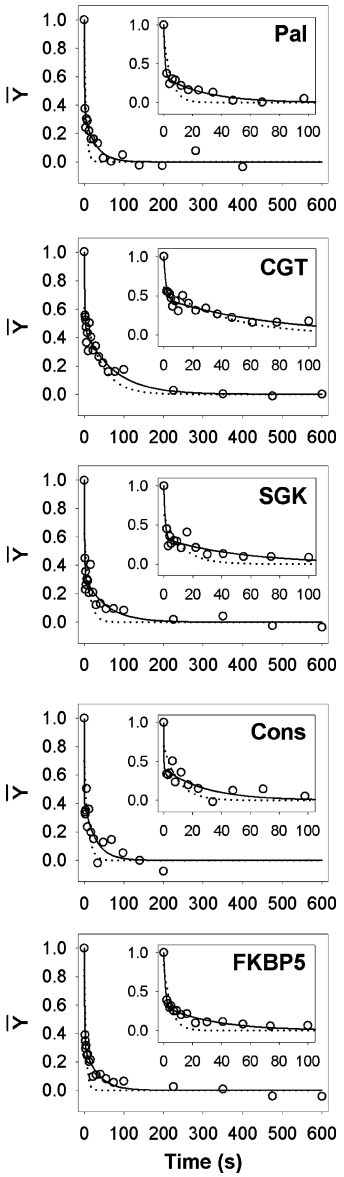

Figure 5. Decay curves for dissociation of GR from five response elements. Empty circles represent time-dependent GR occupancy at each response element. The dotted line represents the best fit to a single-exponential model; the solid line represents a fit to the biphasic decay model. GR concentrations were 0.5 μM for Pal, 0.7 μM for CGT, 0.5 μM for SGK, 0.6 μM for Cons, and 1.1 μM for FKBP5.

times last only seconds to tens of seconds. This seems to be a general result because we observe rapid exchange for full-length GR and a GR chimera, at an array of individual response elements, and at the multisite MMTV promoter. Recent surface plasmon resonance studies of interactions of the GR DBD with response elements are qualitatively consistent with this result, reporting apparent half-lives of ∼20−50 s.[18] Our findings therefore demonstrate that GR exchange with DNA occurs on a similar time scale in both the test tube and live cells. Although this convergence does not necessarily mean that the receptor uses identical DNA binding mechanisms in both environments, it does suggest that additional biophysical studies of GR−DNA interactions *in vitro* should prove to be useful in interpreting receptor−chromatin behavior *in vivo*.

In contrast to the results presented here, early investigations found that GR−DNA residence times lasted minutes to

DOI: 10.1021/acs.biochem.5b00693
Biochemistry 2015, 54, 5306−5314

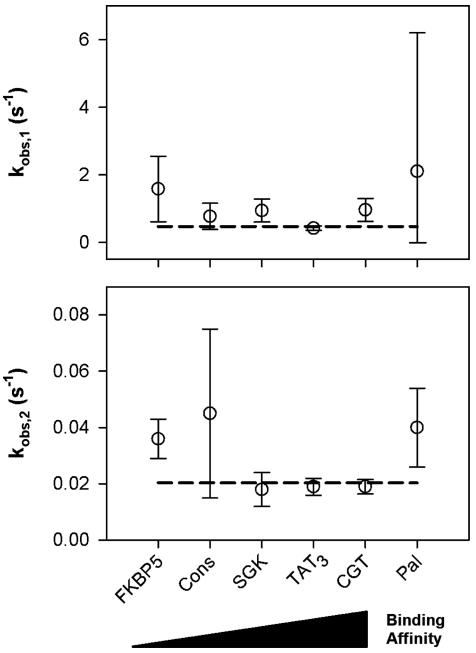

Figure 6. Observed rate constants for dissociation of GR from six response elements. Empty circles represent either $k_{obs,1}$ or $k_{obs,2}$ determined for each sequence by global analysis of at least two decay curves. Error bars represent the standard deviation. The GR binding affinity for the six sequences decreases 80-fold from left to right. The dashed lines represent the weighted average for each rate constant across all response elements. Averages were calculated to be 0.5 ± 0.2 s^{-1} for $k_{obs,1}$ and 0.020 ± 0.006 s^{-1} for $k_{obs,2}$.

Table 2. Observed Rate Constants for Biphasic Dissociation of GR from Six Individual Response Elements[a]

HRE	$k_{obs,1}$ (s^{-1})	$k_{obs,2}$ (s^{-1})
Pal	2.1 (−2.1, +4.1)	0.04 ± 0.01
CGT	1.0 ± 0.3	0.019 ± 0.003
TAT_3	0.4 ± 0.1	0.019 ± 0.003
SGK	0.9 ± 0.3	0.018 ± 0.006
Cons	0.8 ± 0.4	0.05 ± 0.03
FKBP5	1.6 ± 0.9	0.036 ± 0.007

[a]Parameters for each sequence were resolved by globally fitting 2−11 decay curves, covering a range of GR concentrations, to a two-phase exponential decay model using Scientist. Errors represent 68% confidence limits determined via fitting. GR concentrations are as noted in Figure 5.

hours.[4,5] Although the basis of this discrepancy is unclear, we note that at the time of these studies, it was not yet possible to recombinantly express full-length GR. Instead, the receptor was extracted from tissue samples and partially purified in relatively small amounts. Although recombinant expression of the isolated DBD had been achieved, the extent of activity for the purified domain was not always clear. It is thus conceivable that in these early studies, contaminating proteins and/or structural heterogeneity contributed to long residence times.

Association Kinetics Control GR−DNA Binding Affinity. We previously found that for the six response elements shown in Figure 1a, GR binding affinity spanned a 80-fold range.[7] Noting that the off rates for these sequences are essentially identical, this implies that receptor on rate controls binding affinity. This is somewhat surprising because studies of other transcription factors have shown that the off rate is the

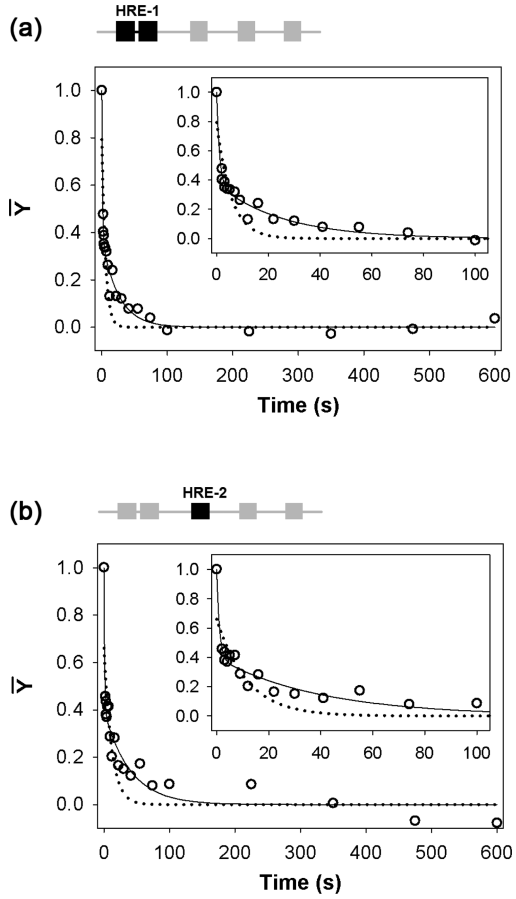

Figure 7. Dissociation of GR from the MMTV promoter and individual decay curves. (a) Schematic and decay curve for dissociation of GR from site 1. The dotted line represents the best fit to a single-exponential decay model. The solid line represents the best fit to a biphasic decay model. Fits covering the first 100 s of dissociation are shown in the inset. (b) Schematic and decay curve for dissociation of GR from site 2. Symbols, lines, and the inset are as described for panel a. The GR concentration was 0.8 μM.

controlling factor.[19,20] However, these studies were conducted using either "simple" repressors or fragments of more complex transcription factors. These examples may not be most appropriate for larger, multidomain proteins such as GR. Better models may instead come from the field of immunology. Kinetic analyses of both antibody−epitope interactions and T cell receptor−peptide interactions have revealed that on rate often controls binding affinity.[21−23] Although the molecular basis for such control is not fully understood, it is thought that rate-limiting structural reorganization in one or both macromolecules must occur upon assembly. Interestingly, both GR and DNA are also known to undergo structural transitions upon binding.[24] Whether these transitions are linked to on rate control of affinity will require detailed studies of the time dependence of GR−DNA association. We expect that these investigations (currently underway) will reveal complex and multiphasic kinetics, with association rate constants comparable to those of other transcription factors (~1 × 10^8 M^{-1} s^{-1}) that decrease as GR−DNA binding affinity weakens.[25]

Biphasic GR−DNA Dissociation Suggests Interconversion between States. Our final observation was that GR−DNA dissociation kinetics are biphasic in character. This indicates that GR does not dissociate in a single step, which

DOI: 10.1021/acs.biochem.5b00693
Biochemistry 2015, 54, 5306−5314

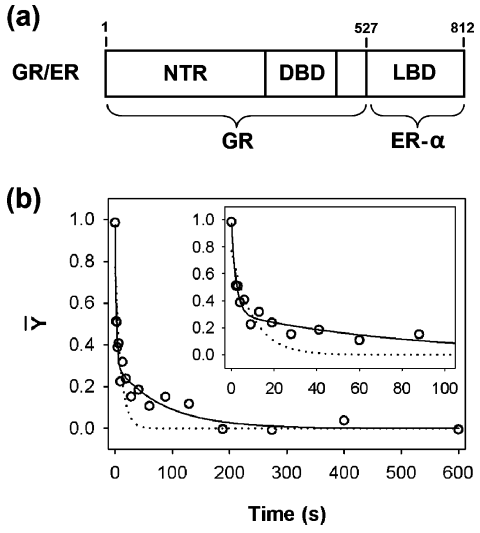

Figure 8. Schematic and decay curve for dissociation of the GR/ER chimera from the TAT_3 sequence. (a) Schematic representation of the GR/ER primary structure. The ligand binding domain of GR is replaced with that of ER-α. Functional domains and regions are as indicated: NTR, N-terminal region; DBD, DNA binding domain; LBD, ligand binding domain. (b) Decay curve for GR/ER–TAT_3 dissociation. Empty circles represent the time-dependent GR/ER occupancy. The dotted line represents the best fit to a single-exponential model; the solid line represents the fit to a biphasic decay model. The GR/ER concentration was 0.7 μM.

would predict a monoexponential decay curve. Instead, dissociation occurs in multiple steps, possibly via an intermediate. Our goal here is to establish a minimal kinetic model to describe this phenomenon. One possibility is that GR monomers sequentially dissociate from the half-sites within a response element. However, this predicts that decay curves generated from each half-site should be different from each other, with one half-site showing rapid decay and the other showing slow decay. However, quantification of each half-site in the footprint shown in Figure 3a generated decay curves identical to each other and to the full-site curve shown in Figure 3b (not shown). Half-site analysis of the remaining response elements also revealed decay curves identical to those for the full sites.

A second possibility is that monomers randomly dissociate via a nonsequential pathway regardless of HRE sequence. Although we cannot formally eliminate this possibility, we think it unlikely for two reasons. First, we note that binding of the GR dimer to the DNA is associated with significant hypersensitivity adjacent to the binding site (Figure 3a); this is presumably due to receptor-induced DNA bending. If so, then hypersensitivity is reporting on the dimer-bound rather than monomer-bound ligation state. If monomers randomly and sequentially dissociate, we would therefore expect to observe a monoexponential decay in hypersensitivity. Instead, quantification of the hypersensitive sites reveals biphasic decay identical to that seen in Figure 3b (not shown). Second, in contrast to our preferred model (described in more detail below), we can think of no obvious biological advantage to random monomer dissociation.

A third possibility is that in the absence of DNA, GR exists as two independent species existing in similar proportions. This might be due to the presence of a truncated or misfolded receptor population generated during purification. However, we would expect that these species would be manifested as heterogeneity in our sedimentation velocity and/or equilibrium footprinting studies, yet we detect a single species by sedimentation velocity and a single binding transition by equilibrium footprinting. Noting that we also observe biphasic kinetics with the GR/ER chimera, we conclude this possibility also seems unlikely.

This led us to the model in Figure 9a, which postulates that the GR–DNA complex reversibly interconverts between two states, A and B, with state A dissociating from the DNA via rate constant $k_{off,A}$. Interconversion between the states is controlled by rate constants k_{AB} and k_{BA}. Using the differential equations that describe this model (eqs 3–5), we globally fit 11 TAT_3 dissociation curves covering a 10-fold range of GR concen-

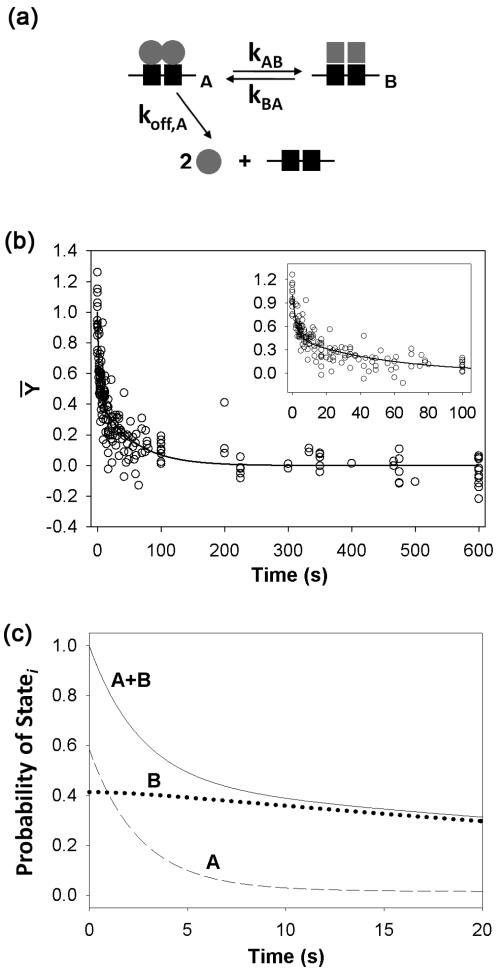

Figure 9. Global analysis of GR–TAT_3 decay curves using a minimal kinetic model. (a) DNA-bound GR interconverts between states A and B via rate constants k_{AB} and k_{BA}. GR dissociates only from state A via dissociation rate constant $k_{off,A}$. Gray circles represent GR monomers, and adjoined black squares represent the response element. (b) Global analysis of 11 decay curves covering a 10-fold range of GR concentrations. Empty circles represent the time-dependent GR occupancy. The solid line represents the best fit by numerical integration of the ordinary differential equations that describe the model (see Materials and Methods). The inset shows the fit to the first 100 s of dissociation. (c) Probability of the two GR–DNA microstates in the first 20 s. The dashed line represents the probability of state A; the dotted line represents the probability of state B. The solid line represents the sum of states A and B and is equivalent to the fit line in panel a.

DOI: 10.1021/acs.biochem.5b00693
Biochemistry 2015, 54, 5306–5314

trations. The resultant fit is shown in Figure 9b, with the time-dependent probability of each DNA-bound state shown in Figure 9c. This latter plot predicts that at equilibrium (t = 0), states A and B exist in comparable proportions, with state A existing at just <60% and state B slightly >40%. With regard to kinetic parameters, the dissociation rate constant for state A, $k_{off,A}$, is 0.4 ± 0.1 s^{-1}, corresponding to an average residence time of 2.5 s. More interesting are the values for isomerization rate constants k_{AB} and k_{BA}. These were found to be 0.020 ± 0.008 and 0.026 ± 0.005 s^{-1}, respectively. These translate to half-lives for each state of approximately 30 s.

Noting that interactions of GR with coactivating proteins also occur on a time scale of seconds to tens of seconds,[26,27] we speculate that receptor interconversion on a similar time scale may be functionally relevant. Similar to arguments made for T cell receptor−peptide interactions,[28,29] it may be that the coactivating proteins and ligands that target GR are capable of distinguishing between the different DNA-bound states, leading to unique transcriptional responses: one possibility is that they reflect the productive versus unproductive transcriptional activation complexes observed in live cells.[30] Alternatively, there may be synchronous cross-talk between receptor interconversion and cyclical chromatin remodeling events.[31] Although further work will be necessary to confirm this thinking, we believe the model in Figure 9a represents the minimal complexity necessary to describe the data. Although other models were consistent with our decay curves, they required additional kinetic parameters or additional phases or suggested no biological relevance, making them unwarranted.

AUTHOR INFORMATION

Corresponding Author

*Address: 12850 E. Montview Blvd., C-238, Department of Pharmaceutical Sciences, University of Colorado Anschutz Medical Campus, Aurora, CO 80045. Phone: 303-724-6118. Fax: 303-724-7266. E-mail: david.bain@ucdenver.edu.

Present Address

§N.K.M.: Alliance Protein Laboratories, Inc., San Diego, CA 92121.

Funding

This work was supported by grants from the National Institutes of Health (DK-88843) and the ALSAM Foundation Skaggs Scholars Program.

Notes

The authors declare no competing financial interest.

ACKNOWLEDGMENTS

We are grateful to Dr. Anne Libby for insightful discussions.

ABBREVIATIONS

GR, glucocorticoid receptor; ER-α, estrogen receptor-α; GR/ER, glucocorticoid-estrogen receptor; DBD, DNA binding domain; HRE, hormone response element; MMTV, mouse mammary tumor virus; TA, triamcinolone acetonide; E2, 17-β-estradiol.

REFERENCES

(1) Tsai, M. J., and O'Malley, B. W. (1994) Molecular mechanisms of action of steroid/thyroid receptor superfamily members. *Annu. Rev. Biochem. 63*, 451−486.

(2) McNally, J. G., Müller, W. G., Walker, D., Wolford, R., and Hager, G. L. (2000) The glucocorticoid receptor: rapid exchange with regulatory sites in living cells. *Science 287*, 1262−1265.

(3) Morisaki, T., Müller, W. G., Golob, N., Mazza, D., and McNally, J. G. (2014) Single-molecule analysis of transcription factor binding at transcription sites in live cells. *Nat. Commun. 5*, 4456.

(4) Perlmann, T., Eriksson, P., and Wrange, O. (1990) Quantitative analysis of the glucocorticoid receptor-DNA interaction at the mouse mammary tumor virus glucocorticoid response element. *J. Biol. Chem. 265*, 17222−17229.

(5) Lieberman, B. A., and Nordeen, S. K. (1997) DNA intersegment transfer, how steroid receptors search for a target site. *J. Biol. Chem. 272*, 1061−1068.

(6) Nagaich, A. K., Walker, D. A., Wolford, R., and Hager, G. L. (2004) Rapid periodic binding and displacement of the glucocorticoid receptor during chromatin remodeling. *Mol. Cell 14*, 163−174.

(7) Bain, D. L., Yang, Q., Connaghan, K. D., Robblee, J. P., Miura, M. T., Degala, G. D., Lambert, J. R., and Maluf, N. K. (2012) Glucocorticoid receptor-DNA interactions: binding energetics are the primary determinant of sequence-specific transcriptional activity. *J. Mol. Biol. 422*, 18−32.

(8) Robblee, J. P., Miura, M. T., and Bain, D. L. (2012) Glucocorticoid receptor−promoter interactions: energetic dissection suggests a framework for the specificity of steroid receptor-mediated gene regulation. *Biochemistry 51*, 4463−4472.

(9) Meijsing, S. H., Pufall, M. A., So, A. Y., Bates, D. L., Chen, L., and Yamamoto, K. R. (2009) DNA binding site sequence directs glucocorticoid receptor structure and activity. *Science 324*, 407−410.

(10) Connaghan, K. D., Miura, M. T., Maluf, N. K., Lambert, J. R., and Bain, D. L. (2013) Analysis of a glucocorticoid-estrogen receptor chimera reveals that dimerization energetics are under ionic control. *Biophys. Chem. 172*, 8−17.

(11) Gill, S. C., and von Hippel, P. H. (1989) Calculation of protein extinction coefficients from amino acid sequence data. *Anal. Biochem. 182*, 319−326.

(12) Schuck, P. (2000) Size-distribution analysis of macromolecules by sedimentation velocity ultracentrifugation and lamm equation modeling. *Biophys. J. 78*, 1606−1619.

(13) Brenowitz, M., Senear, D. F., Shea, M. A., and Ackers, G. K. (1986) Quantitative DNase footprint titration: a method for studying protein-DNA interactions. *Methods Enzymol. 130*, 132−181.

(14) Connaghan-Jones, K. D., Moody, A. D., and Bain, D. L. (2008) Quantitative DNase footprint titration: a tool for analyzing the energetics of protein-DNA interactions. *Nat. Protoc. 3*, 900−914.

(15) Hsieh, M., and Brenowitz, M. (1996) Quantitative kinetics footprinting of protein-DNA association reactions. *Methods Enzymol. 274*, 478−492.

(16) Streaker, E. D., and Beckett, D. (2003) Coupling of protein assembly and DNA binding: biotin repressor dimerization precedes biotin operator binding. *J. Mol. Biol. 325*, 937−948.

(17) Bevington, P. R., and Robinson, D. K. (2003) *Data reduction and error analysis for the physical sciences*, McGraw-Hill, New York.

(18) Watson, L. C., Kuchenbecker, K. M., Schiller, B. J., Gross, J. D., Pufall, M. A., and Yamamoto, K. R. (2013) The glucocorticoid receptor dimer interface allosterically transmits sequence-specific DNA signals. *Nat. Struct. Mol. Biol. 20*, 876−883.

(19) Kim, J. G., Takeda, Y., Matthews, B. W., and Anderson, W. F. (1987) Kinetic studies on Cro repressor-operator DNA interaction. *J. Mol. Biol. 196*, 149−158.

(20) Hart, D. J., Speight, R. E., Cooper, M. a, Sutherland, J. D., and Blackburn, J. M. (1999) The salt dependence of DNA recognition by NF-kappaB p50: a detailed kinetic analysis of the effects on affinity and specificity. *Nucleic Acids Res. 27*, 1063−1069.

(21) Ely, L. K., Green, K. J., Beddoe, T., Clements, C. S., Miles, J. J., Bottomley, S. P., Zernich, D., Kjer-Nielsen, L., Purcell, A. W., McCluskey, J., Rossjohn, J., and Burrows, S. R. (2005) Antagonism of antiviral and allogeneic activity of a human public CTL clonotype by a single altered peptide ligand: implications for allograft rejection. *J. Immunol. 174*, 5593−5601.

DOI: 10.1021/acs.biochem.5b00693
Biochemistry 2015, 54, 5306−5314

(22) Jones, L. L., Colf, L. a., Bankovich, A. J., Stone, J. D., Gao, Y. G., Chan, C. M., Huang, R. H., Garcia, K. C., and Kranz, D. M. (2008) Different thermodynamic binding mechanisms and peptide fine specificities associated with a panel of structurally similar high-affinity T cell receptors. *Biochemistry 47*, 12398−12408.
(23) Zhang, W., Godillot, a. P., Wyatt, R., Sodroski, J., and Chaiken, I. (2001) Antibody 17b binding at the coreceptor site weakens the kinetics of the interaction of envelope glycoprotein gp120 with CD4. *Biochemistry 40*, 1662−1670.
(24) Kumar, R., and McEwan, I. J. (2012) Allosteric modulators of steroid hormone receptors: structural dynamics and gene regulation. *Endocr. Rev. 33*, 271−299.
(25) Halford, S. E., and Marko, J. F. (2004) How do site-specific DNA-binding proteins find their targets? *Nucleic Acids Res. 32*, 3040−3052.
(26) Becker, M., Baumann, C., John, S., Walker, D. A., Vigneron, M., McNally, J. G., and Hager, G. L. (2002) Dynamic behavior of transcription factors on a natural promoter in living cells. *EMBO Rep. 3*, 1188−1194.
(27) Johnson, T. A., Elbi, C., Parekh, B. S., Hager, G. L., and John, S. (2008) Chromatin remodeling complexes interact dynamically with a glucocorticoid receptor-regulated promoter. *Mol. Biol. Cell 19*, 3308−3322.
(28) Anderson, T., and McConnell, H. (1999) Interpretation of biphasic dissociation kinetics for isomeric class II major histocompatibility complex-peptide complexes. *Biophys. J. 77*, 2451−2461.
(29) Rabinowitz, J. D., Liang, M. N., Tate, K., Lee, C., Beeson, C., and McConnell, H. M. (1997) Specific T cell recognition of kinetic isomers in the binding of peptide to class II major histocompatibility complex. *Proc. Natl. Acad. Sci. U. S. A. 94*, 8702−8707.
(30) Métivier, R., Reid, G., and Gannon, F. (2006) Transcription in four dimensions: nuclear receptor-directed initiation of gene expression. *EMBO Rep. 7*, 161−167.
(31) Stavreva, D. A., Varticovski, L., and Hager, G. L. (2012) Complex dynamics of transcription regulation. *Biochim. Biophys. Acta, Gene Regul. Mech. 1819*, 657−666.

DOI: 10.1021/acs.biochem.5b00693
Biochemistry 2015, 54, 5306−5314